

ARTICLE

<https://doi.org/10.1038/s42003-019-0386-6>

OPEN

Secreted parasite Pin1 isomerase stabilizes host PKM2 to reprogram host cell metabolism

Justine Marsolier^{1,2}, Martine Perichon¹, Jonathan B. Weitzman^{1,3} & Souhila Medjkane^{1,3}

Metabolic reprogramming is an important feature of host–pathogen interactions and a hallmark of tumorigenesis. The intracellular apicomplexa parasite *Theileria* induces a Warburg-like effect in host leukocytes by hijacking signaling machineries, epigenetic regulators and transcriptional programs to create a transformed cell state. The molecular mechanisms underlying host cell transformation are unclear. Here we show that a parasite-encoded prolyl-isomerase, TaPin1, stabilizes host pyruvate kinase isoform M2 (PKM2) leading to HIF-1 α -dependent regulation of metabolic enzymes, glucose uptake and transformed phenotypes in parasite-infected cells. Our results provide a direct molecular link between the secreted parasite TaPin1 protein and host gene expression programs. This study demonstrates the importance of prolyl isomerization in the parasite manipulation of host metabolism.

¹Sorbonne Paris Cité, Epigenetics and Cell Fate, Université Paris Diderot, CNRS, UMR 7216 Paris, France. ²Present address: Institut Curie, 26 rue d’Ulm, 75005 Paris, France. ³These authors contributed equally: Jonathan B. Weitzman, Souhila Medjkane. Correspondence and requests for materials should be addressed to J.B.W. (email: jonathan.weitzman@univ-paris-diderot.fr) or to S.M. (email: souhila.medjkane@univ-paris-diderot.fr)

The metabolic switch to aerobic glycolysis is an important characteristic of tumorigenesis and cellular reprogramming^{1,2}. Metabolic exchange is also a key factor in parasite–host interactions and the manipulation of host cell phenotypes. Several parasites enter into intricate metabolic exchange with their host cells³. *Theileria* parasites are remarkable for their ability to interfere with host signaling pathways, activate nuclear transcription factors (e.g., c-Myc, HIF1 α , and AP-1) and transform host leukocytes^{4–7}. We previously described a Warburg-like phenotype in infected leukocytes associated with stabilization of hypoxia induced factor 1 α (HIF1 α) and induction of aerobic glycolytic genes^{4,8,9}. We also discovered that *Theileria* parasites secrete a Peptidyl-prolyl isomerase (TaPin1) into the host cell, which induces proliferation via the host transcription factor c-Jun¹⁰. We found that TaPin1 is targeted by the theilericidal drug Buparvaquone, though there may be additional pathways targeted by this drug. In this study, we set out to identify molecular mechanisms that could link the secreted parasite TaPin1 protein to host signaling pathways. We show that TaPin1 interacts with the host Pyruvate Kinase Isoform M2 (PKM2), leading to its stabilization and subsequent HIF1 α -dependent induction of glycolytic enzymes that contribute to host transformed phenotypes.

Results

Parasite TaPin1 stabilizes host PKM2 protein. To search for Pin1 interactors, we expressed ectopic, tagged Pin1 in fibroblasts and performed immunoprecipitation followed by mass spectrometry analysis (Supplementary Fig. 1a). We identified several potential interacting proteins in the cytoplasm. This list of interacting proteins is unlikely to be exhaustive, as the previously identified FBW7 protein was not found in this screen¹¹. One of the most abundant Pin1-interactors was PKM2 (Supplementary Data 1). We investigated whether GST-TaPin1 could also interact with host PKM2 in extracts from bovine leukocyte cell lines infected with either *T. annulata* or *T. parva*. (Fig. 1a). To confirm this interaction, we transfected Flag-tagged PKM2 into TBL3 infected cells and showed that it interacts with the endogenous parasite TaPin1 protein (Fig. 1b). To examine the consequences of the TaPin1–PKM2 interaction, we monitored the levels of the endogenous PKM2 protein in parasite-infected TBL3 cells, compared to non-infected BL3 cells (Fig. 1c) and observed elevated levels in parasitized cells. Furthermore, treatment with two pharmacological PPIase inhibitors, Buparvaquone or Juglone¹⁰, led to a reduction in the PKM2 protein levels in TBL3 parasitized cells (Fig. 1d and quantification in Supplementary Fig. 1b). Treatment with Buparvaquone or Juglone had no effect on the levels of PKM2 mRNA in parasitized TBL3 cells (Supplementary Fig. 1c). Inhibition of TaPin1 with Buparvaquone or Juglone or ectopic expression of TaPin1 did not change basal PKM2 protein levels in control BL3 cells (Supplementary Fig. 1b, d). It could be that BL3 cells lack effectors required for the TaPin1 effects. To test whether parasite TaPin1 could regulate bovine PKM2 protein stability, we investigated PKM2 ubiquitination and half-life. We found that Buparvaquone/Juglone treatment induced the ubiquitination of PKM2 (Fig. 1e) and reduced the half-life of PKM2 in parasitized TBL3 cells (Fig. 1f and Supplementary Fig. 1e) as measured by cycloheximide pulse-chase experiments. Together these results showed that the *Theileria* parasite TaPin1 prolyl isomerase interacts (directly or indirectly) with host bovine PKM2 and leads to its stabilization.

Parasite TaPin1 regulates host cell metabolism. In addition to its role in phosphoenolpyruvate phosphorylation, PKM2 acts as a cofactor for HIF1 α , a transcription factor critical for the Warburg

effect and the transcription of glycolytic enzymes in cancer cells^{12–14}. We tested whether stabilization of host PKM2 by the parasite TaPin1 protein could affect HIF1 α functions. We observed that TaPin1 inhibition (via Buparvaquone or Juglone treatment) reduced transcriptional activity of HIF1 α (40–50%), measured by a hypoxia-responsive element (5 \times HRE) Luciferase reporter (Fig. 2a). The reduced HIF1 α activity correlated with reduced expression of HIF1 α -target genes linked to host cell metabolism, namely genes encoding the glycolytic enzymes Hexokinase 2 [HKII], the Glucose transporter 1 [GLUT1], Pyruvate dehydrogenase kinase [PDK1] and Lactate dehydrogenase [LDHA]. The expression of HIF1 α -target genes was reduced at the mRNA level (40–70%) (Fig. 2b) and protein levels (Fig. 2d). The PPIase inhibitors had no effect on the expression of HIF1 α transcripts (Fig. 2b). Experiments in control BL3 cells indicated that Buparvaquone or Juglone treatment did not affect the expression of glycolytic enzymes in unparasitized cells (Supplementary Fig. 2a). To show that the regulation of metabolic enzymes could be via parasite TaPin1-dependent stabilization of host PKM2 protein, we transfected exogenous PKM2 into TBL3 cells prior to treatment with TaPin1 inhibitors. The forced expression of PKM2 rescued expression of the metabolic enzymes (GLUT1, LDHA, and PDK1) in the presence of Juglone inhibitor (Fig. 2c). Conversely, siRNA silencing of endogenous, bovine PKM2 reduced HIF1 α -activity using the 5xHRE luciferase reporter assay in TBL3 cells (Fig. 2e, f). This correlated with a marked reduction in the expression of host glycolytic enzymes without affecting the levels of HIF1 α transcripts in TBL3 cells (Fig. 2g). Notably, siRNA directed against PKM2 did not decrease the expression of the glycolytic enzymes in control BL3 cells (Supplementary Fig. 2b, c).

Parasite TaPin1 can partially rescue PKM2 regulation. To provide further support for a role of TaPin1–PKM2 in the regulation of host metabolic enzymes, we tested TaPin1's ability to rescue the Buparvaquone effects. Overexpression of TaPin1 could partially rescue the expression of PKM2 proteins in TBL3 cells treated with Buparvaquone (Fig. 3a) leading to a partial rescue of the expression of glycolytic enzymes (Fig. 3b). To demonstrate the importance of the prolyl isomerase activity, we tested TaPin1-K38A and TaPin1-S42E catalytic mutants^{10,15}. These failed to rescue PKM2 stabilization or glycolytic enzyme expression (Supplementary Fig. 3a, b). We previously reported a mutation in the parasite *TaPin1* gene that resulted in a Buparvaquone-resistant protein¹⁰. Interestingly, transfection experiments in TBL3 cells showed that the TaPin1-A53P mutant was not sensitive to Buparvaquone effects on PKM2 protein levels (Fig. 3c) and the expression of the glycolytic enzymes in TBL3 cells (Fig. 3d). The TaPin1-A53P mutant remains sensitive to the Juglone drug¹⁰ and failed to maintain PKM2 protein levels in Juglone-treated TBL3 cells (Fig. 3c) or glycolytic enzyme expression (Fig. 3d). Finally, we performed knockdown experiments to exclude a role for the endogenous bovine Pin1 protein in regulating PKM2 and metabolic enzymes in TBL3 cells. We tested siRNA knockdown of endogenous bovine *Pin1* and showed that siBtPin1 did not affect PKM2 protein expression (Supplementary Fig. 4a) or HIF1 α -target gene expression (Supplementary Fig. 4b). These combined data support a role for the secreted TaPin1 protein in regulating host gene expression through prolyl isomerase stabilization of host PKM2 and the HIF1 α pathway.

The TaPin1–PKM2 axis is important for glucose uptake and host cell transformation. To test the functional significance of TaPin1–PKM2 signaling on host transformation, we measured the effects of TaPin1 inhibitors on glucose uptake in parasitized

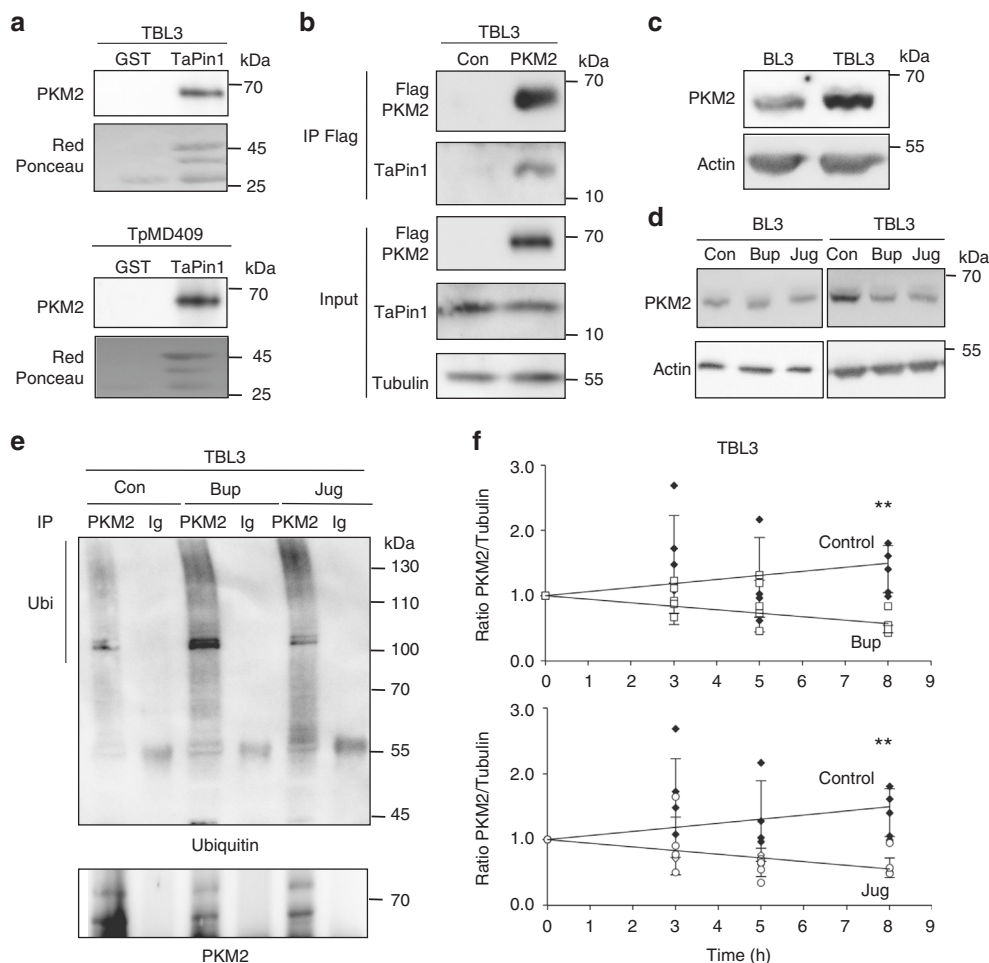


Fig. 1 Parasite TaPin1 stabilizes host PKM2 protein. **a** Recombinant GST-TaPin1 protein interacted with endogenous bovine PKM2 protein in whole-cell lysates from lymphocyte cell lines infected with *T. annulata* (TBL3) or *T. parva* (TpMD409). Original blot images are shown in Supplementary Fig. 7a. **b** Flag-PKM2 interacted with endogenous TaPin1 protein in infected TBL3 cells. Flag-PKM2 or Flag-Control [Con] were immunoprecipitated (IP), followed by immunoblot analysis with indicated antibodies. Original blot images are shown in Supplementary Fig. 7b. **c** Bovine PKM2 protein expression in uninfected BL3 and infected TBL3 cells (bovine Beta-actin was a loading control). Original blot images are shown in Supplementary Fig. 7c. **d** TaPin1 inhibition by Buparvaquone [Bup] or Juglone [Jug] decreased host PKM2 protein levels compared to untreated control [Con] in *T. annulata* infected TBL3 cells but had no effect on uninfected BL3 cells. Original blot images are shown in Supplementary Fig. 7d. **e** Buparvaquone [Bup] or Juglone [Jug] treatment increased host PKM2 protein ubiquitination in infected cells. Infected cells were incubated with the proteasome inhibitor MG132 for 3 h in the presence of Buparvaquone [Bup], or Juglone [Jug] or no inhibitor [Con]. Cell extracts were immunoprecipitated [IP] using antibodies against PKM2 or controls [Ig], followed by immunoblot analysis. **f** TaPin1 inhibition decreased the half-life of endogenous PKM2 protein. TBL3 cells were incubated with cycloheximide and Bup or Jug, followed by immunoblot analysis with a PKM2 antibody and quantification compared to tubulin expression. Data represent four independent experiments (average \pm sd). The *p*-values were calculated using the Dunnett test for multiple comparisons with the control conditions. ***p* < 0.01

cells. Parasitized TBL3 cells exhibited a 9-fold increase in glucose uptake compared to control BL3 cells (Fig. 4a). This parasite-induced effect was reduced by treatment with Juglone or Buparvaquone (Fig. 4a) with no effect in BL3 cells. As demonstrated above for PKM2 stabilization and glycolytic enzyme expression, the Buparvaquone and Juglone effects on glucose uptake could be partially rescued by overexpression of ectopic PKM2 in TBL3 cells (Fig. 4b, c). Furthermore, knockdown of endogenous PKM2 in parasitized cells also led to a reduction in glucose uptake (Fig. 4d). Notably, the overexpression of ectopic PKM2 or siRNA-mediated knockdown PKM2 did not affect the glucose uptake of control BL3 cells (Supplementary Fig. 2d and Fig. 4d). Finally, we tested the contribution of TaPin1 and PKM2 to the transformed phenotype of parasitized cells. Treatment of parasite-infected TBL3 cells with TaPin1 inhibitors, Juglone or

Buparvaquone, or knockdown of endogenous PKM2, each led to a marked decrease in cell proliferation (Supplementary Fig. 5a, b) and the growth of colonies in soft agar, an effective in vitro assay for transformation (Fig. 4e, f). Once again, siPin1 knockdown of bovine *Pin1* did not affect colony growth of TBL3 cells (Supplementary Fig. 4c). These combined experiments suggest that the stabilization of host bovine PKM2 protein by the secreted parasite TaPin1 PPIase leads to activation of HIF1 α -dependent metabolic genes that are essential for glucose metabolism and host cell transformation.

Discussion

Metabolic reprogramming is a hallmark of cancer cells and is critical for tumor cell survival and proliferation^{2,16}. Previous

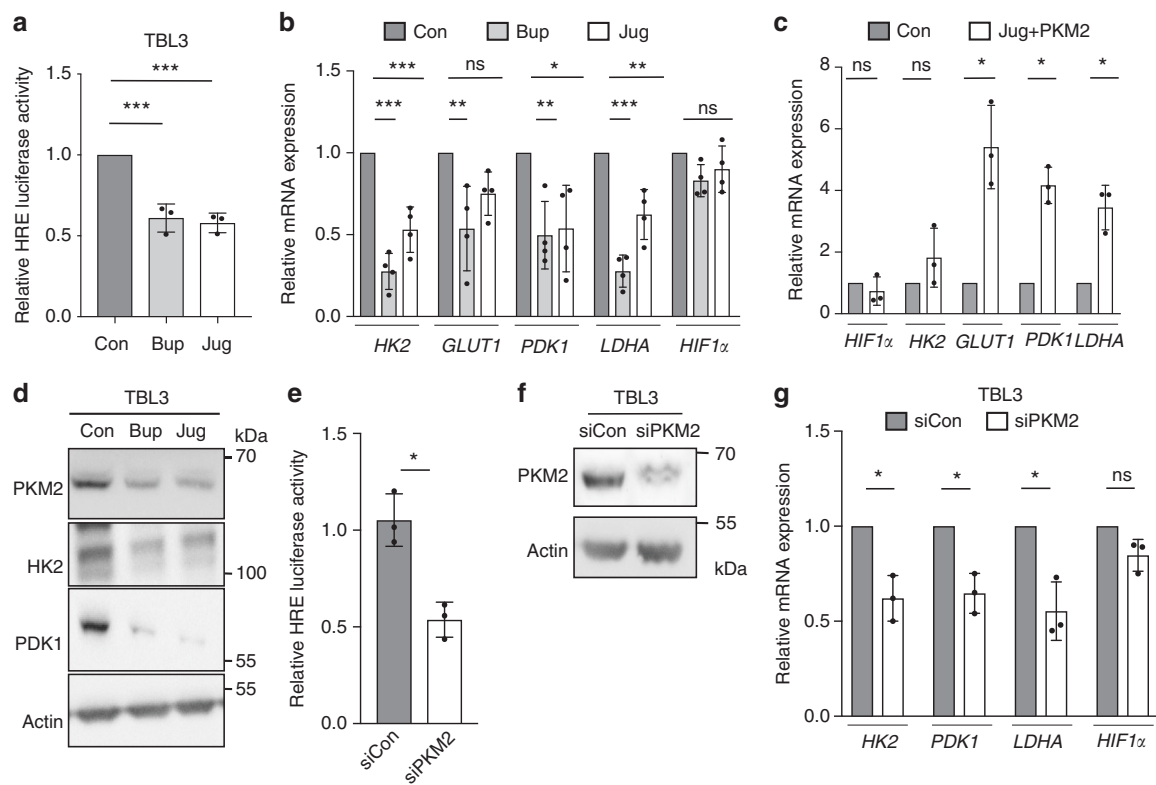


Fig. 2 Parasite TaPin1 regulates host HIF1 α activity and metabolic gene expression. **a** TaPin1 inhibition with Buparvaquone/Juglone treatment decreased the activity of a 5 \times HRE HIF1 α Luciferase reporter. **b** TaPin1 inhibition decreased the expression of HIF1 α target genes in TBL3 cells. qPCR analysis of host gene expression upon TaPin1 inhibition by Buparvaquone or Juglone compared to untreated controls [Con]. Bovine Beta-actin and H2A mRNAs were used for normalization. **c** Ectopic expression of PKM2 in parasite-infected TBL3 cells rescued the repression of host glycolytic enzymes observed upon TaPin1 inhibition with Juglone treatment. **d** TaPin1 inhibition decreased the expression of glycolytic enzyme proteins. (Bovine Beta-actin was a loading control). Original blot images are shown in Supplementary Fig. 7e. **e** siPKM2 decreased HIF1 α activity on 5xHRE Luciferase reporter. **f** Efficiency of siPKM2. Bovine Beta-actin was used as a loading control. Original blot images are shown in Supplementary Fig. 7f. **g** PKM2 knockdown decreased the mRNA levels of the HIF1 α targets (siPKM2 or siControl). Bovine Beta-actin and H2A mRNAs were used for normalization. Data represent three independent experiments (average \pm sd). The *p*-values were calculated using the Dunnett test for multiple comparisons (Fig. 2a, b). The *p*-values were calculated using the Mann-Whitney test (Fig. 2c-f). **p* < 0.05, ***p* < 0.01, ****p* < 0.001

reports of Warburg-like “aerobic glycolysis” in bovine leukocyte cell lines transformed by *Theileria* parasites^{17,18} lacked a direct molecular link between intracellular parasites and host metabolic gene expression. Here, we identified the TaPin1–PKM2–HIF1 α axis as an integrator of parasite–host interaction. We showed that TaPin1 and bovine PKM2 interact (either directly or indirectly) and that this interaction leads to PKM2 stabilization and HIF1 α -dependent glycolytic enzyme expression.

PKM2 plays a critical role in the metabolic rewiring that underlies tumorigenesis¹⁹. Non-canonical PKM2 functions include nuclear transcriptional regulation^{12–14,20} and enhanced HIF1 α binding to HRE in metabolic genes^{13,14}. The PKM2 protein is finely tuned by cancer cells, involving mRNA splicing, ERK-dependent phosphorylation, and subcellular relocalization. We propose prolyl isomerization and protein stabilization as another level of regulation that parasites exploit to maintain a Warburg-like phenotype. These data add to the descriptions of the complex metabolic relationships between parasites and their host cells³. Increased glucose flux and energy metabolism could support the biosynthetic requirements of both the parasite and the hyperproliferating host cell. The secreted parasite TaPin1 protein could activate multiple pathways that are important for host cell proliferation and metabolism. For example, TaPin1 stabilizes the host transcription factor c-Jun by regulating a ubiquitin ligase, FBW7¹⁰. Additional secreted proteins may

contribute to subverting the host cell and perhaps TaPin1 has additional targets. Here, we show that TaPin1 also activates HIF1 α -regulated target genes via stabilization of PKM2. These results provide a molecular link between prolyl isomerization and metabolic manipulation by intracellular parasites.

Methods

Cell lines and culture conditions. All infected bovine cell lines were previously described: the TBL3 cell line was derived from in vitro infection of the spontaneous bovine-B lymphosarcoma cell line, BL3, with Hissar stock of *T. annulata*. The TpMD409 lymphocyte cell line is infected with *T. parva*. The culture conditions of these cell lines were described previously¹⁰. Parasite-infected cell lines were provided by the Langsley laboratory. Cells were cultured in a humidified 5% CO₂ atmosphere at 37 °C in RPMI 1640 (Gibco-BRL), supplemented with 4 mM L-Glutamine, 25 mM HEPES, 10 μ M Beta-mercaptoethanol, 10% heat-inactivated Fetal calf serum and 100 μ g/ml penicillin/streptomycin. All cell lines were mycoplasma negatives. The anti-parasite drug Buparvaquone (BW720c) was used for 72 h at 200 ng/ml (Chemos GmbH, Ref: 88426-33-9) (Supplementary Fig. 5a, b). Cells were treated 72 h with Juglone at 5 μ M resuspended in Ethanol (Sigma, Ref: H47003).

Plasmids and transfection. Bovine PKM2 (NM_001205727/NP_001192656.1) was cloned between restriction sites *HindIII* and *EcoRI* in p3xFlag-myc-CMV-24 using the following oligonucleotides: Fwd—cccaagcttccgaagcaccacagcgacg and Rev—CGGAATTCGAtggcacaggaactacag. Parasite gene TaPin1 (TA18945) was cloned between restriction sites *XhoI* and *NotI* in pREV-HA-Flag-RIL2 using oligonucleotides: Fwd—CCGCTCGAGGCCCACTTGCTACTAAAG and Rev—ATAAGAATCGCGCCGCTTATGCGATTCTATATATAAGATG. Point

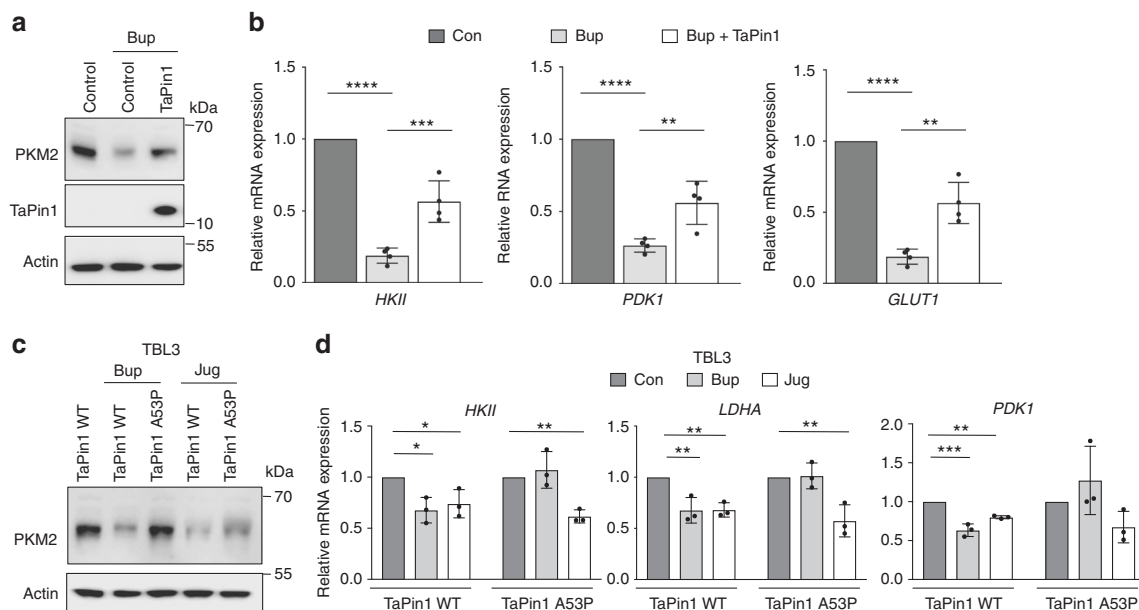


Fig. 3 Parasite TaPin1 can partially rescue PKM2 regulation and glycolytic gene expression in TBL3 cells. **a** Flagged-TaPin1 could partially rescue decreased PKM2 protein levels upon Buparvaquone treatment. Bovine Beta-actin was the loading control. Original blot images are shown in Supplementary Fig. 7g. **b** TaPin1 could partially rescue the expression of HIF1 α target genes upon Buparvaquone treatment. Bovine Beta-actin was used for normalization. **c** Mutant TaPin1-A53P, but not WT TaPin1, is resistant to Buparvaquone effects on PKM2 protein expression in *T. annulata* infected TBL3 cells. Bovine Beta-actin was the loading control. **d** Analysis of bovine glycolytic enzyme gene expression by qPCR in TBL3 cells following Buparvaquone [Bup] or Juglone [Jug] treatment and simultaneous transfection of TaPin1 WT or Mutant A53P. Bovine Beta-actin mRNA was used for normalization. Original blot images are shown in Supplementary Fig. 7h. Data represent three or four (Fig. 3b) independent experiments (average \pm sd). The *p*-values were calculated using the Bonferroni test for multiple comparisons (Fig. 2b) and Dunnett test for multiple comparisons to the control (Fig. 2d). Con, control. ***p* < 0.01, ****p* < 0.001, *****p* < 0.0001

mutations TaPin1 K38A, A53P¹⁰ and S47E were created from pRev-HA-Flag-TaPin1 WT-RIL2 using a set of primers following a 3-step PCR using the following oligos:

Name	Sequence Fwd 5'-3'	Sequence Rev 5'-3'
HsPin1	CCGCTCGAGGCGACGAGGAGAAGCTG	AAGGAAAAAAGCGCCGCT
TaPin1	CCGCTCGAGGCCACTGTACTAAAG	CCTCAGTCCGAGGATGA
TaPin1 K38A	GCCCACTGTCTACTAGCGCACACTGGATCTAGG	ATAAGAATGCGGCCGCTT
TaPin1 S47E	CTAAAGCACACTGGAGAGGAAATCCAGT	ATGCGATTCTATATAAGATG
TaPin1 GST	CGCGGATCCGCCACTGTCTACTAAAG	CCTAGATCCAGTGTGCGTA
PKM2 bov	CCCAAGCTTTCGAAGCACCACGCGACG	GTAGCAAGTGGGC

TBL3 and TBL3 cells were transfected with indicated plasmids using Neon Transfection kit (Invitrogen)¹⁰. Cells were single or double transfected with 400 nM of siRNA. Ectopic PKM2, TaPin1 WT and mutants were transfected between 24 and 36 h after drug treatment.

Name	Sequence Fwd 5'-3'
BtPKM2	TTGTTTCGAGGAGCTCCGCTCC
BtPin1	GCCATTTGAAGACGCTCC

RNA extraction and reverse transcription-qPCR. Total cellular RNAs were extracted using a NucleoSpin RNA Kit (Macherey Nagel, Ref: 740955). cDNA synthesis was performed using the Reverse Transcriptase Superscript III (Invitrogen, Ref: 18080051). Quantitative PCR amplification was performed in the ABI 7500 machine (Applied Biosystems) using the Sybr Green reagent (Applied Biosystems, Ref: 4309155). The detection of a single product was validated by dissociation curve analysis. The bovine Beta-actin and H2A qPCR were used for normalization. Relative quantities of mRNA were analyzed using the delta Ct method.

Name	Sequence Fwd 5'-3'	Sequence Rev 5'-3'
HKII	CGACCAAGTGCAGAAGGTTG	CGTCTGGAGTAGACCTCAC
GLUT1	CATGGAGCCCACCAGCAAG	CGTTGATGACTCCAGTGTG
LDHA	GGCTACACATCCTGGGCC	GGAACACTAAGGAAGACATCC
PDK1	CTAGGCGTCTGTGTGATTG	GATAGAGGTGGGATGGTAC
HIF1a	CATGTGACCACGAGGAAATG	TAGTTCTCCCCGGCTAGTT
PKM2	CCATTACCAGCGACCCAC	GTATCTGGCCACCTGATGTG
H2A	GTCGTGGCAAGCAAGGAG	GATCCGGCCGTTAGGTACTC
BETA-ACTIN	GGCATCCTGACCCTCAAGTA	CACACGGAGTCTCGTTGTAGA

Immunoblot analysis and immunostaining. Total proteins were extracted with Laemmli lysis buffer. Samples were sonicated: 30 s ON/30 s OFF for 5 min, and then resolved on 10.5% acrylamide/bis-acrylamide SDS-PAGE gels and transferred to nitrocellulose membranes (Thermo Fisher Scientific, MA, USA) in transfer buffer. Protein transfer was assessed by performing a Ponceau-red staining. Membranes were then blocked for 1 h at room temperature in Tris-buffered saline pH 7.4 containing 0.1% Tween-20 and 5% milk. Incubations with primary antibodies were performed at 4 °C overnight using antibody dilutions as manufacturer recommendations in Tris-buffered saline pH 7.4, 0.05% Tween-20 and 5% milk. Proteins were detected by chemiluminescence (Thermo Fisher Scientific) following the manufacturer's instructions following 1 h incubation at room temperature with an anti-rabbit or anti-mouse peroxidase-conjugated secondary antibody (Jackson ImmunoResearch, Ref: 111-035-003 or Ref: 115-035-003). We used these antibodies: Rabbit anti-TaPin1 (Home-made antibody, Proteogenix, Peptide used: NPVNRNTGMAVTR-Cys—Dilution 1/100), mouse anti- α Tubulin (Sigma, Ref: T9026—Dilution 1/1000), rabbit anti-PDK1 (C47H1n Cell signaling—Dilution 1/500), rabbit anti-Hexokinase II (Cell Signaling, Ref: C64G5—Dilution 1/500), rabbit anti-PKM2 (Abcam, Ref: ab38237—Dilution 1/250), mouse anti-Beta-actin (Sigma, Ref: A1978—Dilution 1/1000), mouse anti-ubiquitin (P4D1, Ref: sc-8017 Santa Cruz Biotechnology Inc.—Dilution 1/200) and monoclonal anti-Flag M2-Peroxidase (Sigma, Ref: A8592—Dilution 1/1000).

Cycloheximide chase assay. This was performed as previously reported¹⁰. Briefly, after 72 h of treatment with Buparvaquone or Juglone, infected bovine cell line (TBL3) was treated 30, 60, or 120 min with 100 mg/ml Cycloheximide. Cells were

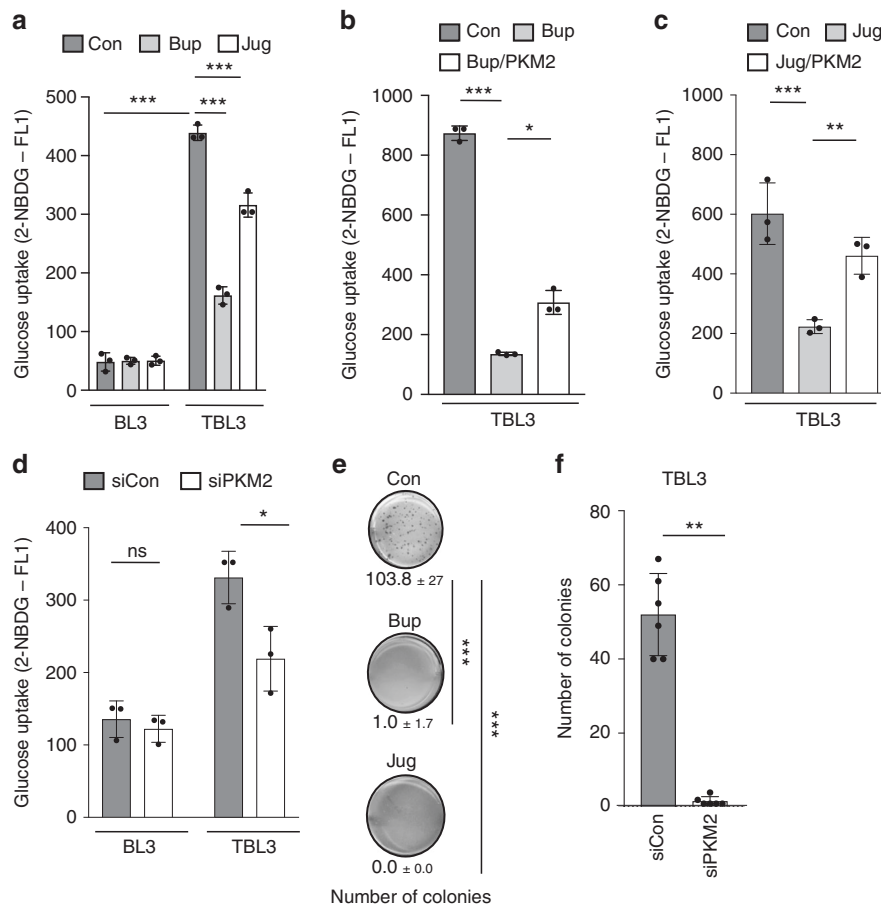


Fig. 4 The TaPin1-PKM2 axis is important for glucose uptake and transformation. **a** Glucose uptake (fluorescence intensity) decreased in *Theileria*-infected TBL3 cells upon TaPin1 inhibition by Buparvaquone or Juglone drugs. **b, c** Ectopic bovine PKM2 partially rescued glucose uptake following TaPin1 inhibition with Buparvaquone (**b**) or Juglone (**c**) in TBL3 cells. **d** PKM2 knockdown reduced glucose uptake in parasitized TBL3 cells (Fluorescence intensity). **e** Inhibition of TaPin1 by Buparvaquone or Juglone affected TBL3 colony formation in soft-agar. **f** siPKM2 reduced TBL3 cell colony formation in soft agar. Data represent three independent experiments (average ± sd). The *p*-values were calculated using the Bonferroni test for multiple comparisons (**a–e**) and the Mann-Whitney test (**f**). **p* < 0.05, ***p* < 0.01, ****p* < 0.001

lysed using Laemmli sample buffer, resolved by SDS-PAGE and analyzed by western blot using the indicated antibodies. Relative quantification indicates the PKM2/ Tubulin ratios calculated with Image J software (NIH) and PKM2 levels at time 0 was set as 1. Cycloheximide chase experiments were repeated for four independent biological replicates.

Viability assays. After plating 1×10^4 cells in 96-well plates in triplicate and Buparvaquone, Juglone was added. After 72 h of treatment, cell viability was measured using the Cell proliferation Kit II-XTT (Roche, measurement of the cellular redox potential) and the GloMax-Multi Detection System (Promega). Cell numbers, as judged by Trypan Blue exclusion test, were determined by counting cells using a Countess automated cell counter (Invitrogen).

Luciferase assay. Bovine cells were transfected with indicated siRNA and the *HRE* Luciferase reporter, using electroporation (Neon kit, Invitrogen, Ref: MPK1096). Transfection efficiencies were normalized to Renilla activity by co-transfection of the reporter plasmid pRL-TK *Renilla* (Promega, Ref: E6241). Luciferase assays were performed using the Dual-Luciferase Reporter Assay System (Promega, Ref: E1980) in a microplate luminometer, 36 h post-transfection. Relative luminescence was represented as the ratio Firefly/Renilla luminescence, compared with the corresponding empty vector control.

Soft agar colony forming assay. A two-layer soft agar culture system was performed. A total of 20,000 bovine cells (treated with Buparvaquone or Juglone) or 40,000 bovine cells (transfected with siRNA) were plated in a volume of 1.5 ml (0.7% SeaKem ME Agarose; Lonza, Ref: 50011 + 2× DMEM 20% Fetal calf Serum over 1.5-ml base layer (1% SeaKem ME Agarose + 2× DMEM 20% Fetal calf Serum) in 6-well plates. Cultures were monitored for growth using a microscope. At the time of maximum colony formation (10–15 days in culture), after fixation a

staining with 0.005% Crystal Violet (Sigma, Ref: C3886) final colony numbers were counted manually.

Measurement of glucose uptake. Cells were incubated in media supplemented with the fluorescent D-glucose analog 2-NBDG (2-[N-(7-nitrobenz-2-oxa-1,3-diazol-4-yl) amino]-2-deoxy-D-glucose, Life Technologies, Ref: N13195) at 100 μM for 20 min at 37 °C. After two washing with PBS, cells were analyzed by flow cytometry, fluorescence assessed in FL1 channel. For each measurement, data from 20,000 single cell events was collected (Supplementary Figure 6) using a FACScalibur flow cytometer (Becton Dickinson Immunocytometry Systems).

GST pull-down. This was performed as previously reported¹⁰. Briefly, TaPin1 and hPin1 were cloned between restriction sites *Bam*HI and *Eco*RI in pGEX-2T plasmid which was kindly provided by G. Del Sal (LNCIB—Laboratorio Nazionale CIB, Trieste, Italy). Plasmid constructs were expressed in *E. coli* strain BL21 and then purified using glutathione-sepharose beads. Concentration of purified protein was estimated using Coomassie blue staining. One microgram of GST fusion proteins coated beads were incubated with 250 μl of cell lysate in 50 mM Tris pH7.6, 150 mM NaCl, 0.1% Triton, for 2 h at 4 °C. Beads were washed five times with 50 mM Tris pH7.6, 300 mM NaCl, 0.5% Triton. Proteins were then revealed by Western Blot analysis using indicated antibodies.

Complex immunopurification and mass spectrometry analysis. We used retroviral transduction strategy to establish NIH/3T3 cell lines expressing double-tagged proteins. Polyclonal NIH/3T3 cell lines stably expressing Flag-HA-tagged hPin1 or TaPin1 were established. All the proteins were tagged with double-HA (Haemagglutinin) and double-Flag epitopes at the N-terminus. A control cell line transduced with the empty pREV vector was established. We carried out double-affinity purification of Flag-HA-hPin1 from NIH/3T3, using either nuclear soluble or cytoplasmic fractions. Both fractions were then subjected to a two-step

immunopurification with Flag and HA antibodies as described previously²¹. Mass spectrometry identification of proteins was carried out in the Taplin Biological Mass Spectrometry Facility (Harvard Medical School, Boston, USA) and the results are shown in Supplementary Data 1.

Immunoprecipitation—HA. TBL3 transiently expressing PKM2 construct were lysed in the following buffer: 20 mM Tris HCL pH8, 150 mM NaCl, 0.6% NP-40 and 2 mM EDTA. Protein complexes were then affinity-purified on anti-Flag antibody-conjugated agarose (Sigma, Ref: A2220) for bovine lysates. Elution was performed using Flag peptide. After five washes, immunopurified complexes were resolved on 4–12% SDS-PAGE bis-Tris acrylamide gradient gel in MOPS buffer (Invitrogen, Ref: NP 0322 BOX, NP0001-02, respectively).

Immunoprecipitation—Ubiquitin. This was performed as previously reported¹¹. Briefly, after 3 h of treatment with 20 μM MG132 at 37 °C, cells were lysed 10 min on ice in the following buffer: 150 mM NaCl, 1% Nonidet P-40, 0.5% Deoxycholate, 0.1% SDS, 50 mM Tris HCl pH 7.5, 20 mM NEM, 5 mM Iodoacetamide, 100 μM MG132, 2 mg/ml Pefabloc SC (Roche) and 5 μg/ml each Aprotinin, Leupeptin, Pepstatin. Equal amounts of total cellular proteins were immunoprecipitated for 90 min at 4 °C with rabbit Anti-PKM2 (Abcam, Ref: 38237) coupled to protein G sepharose beads (Sigma, Ref: P3296). After three washes, immunoprecipitated proteins were eluted at 95 °C for 5 min in Laemmli sample buffer, resolved by SDS-PAGE and analysed by Western blot using the indicated antibodies. Immunoprecipitation was repeated for three independent biological replicates.

Data and statistical analysis. The GraphPad PRISM 7 was used for statistics. In all the figures the results represent the mean ± sd of at least three independent experiments. Statistical analysis was performed using the Dunnett for multiple comparisons with the control condition or Bonferroni test for multiple comparisons between samples or Mann–Whitney test for the comparison between two conditions. *p* values of <0.05 were considered statistically significant and are indicated with asterisks **p* < 0.05; ***p* < 0.01; ****p* < 0.001, *****p* < 0.0001.

Reporting summary. Further information on experimental design is available in the Nature Research Reporting Summary linked to this article.

Data availability

All data generated or analysed during this study are included in this published article, Supplementary Information, and Supplementary Data 1. The list of hPin1 protein interactors identified in this study is included in the Supplementary Data 1. The mass spectrometry proteomics data have been deposited to the ProteomeXchange Consortium via the PRIDE partner repository with the dataset identifier PXD012895.

Received: 29 June 2018 Accepted: 5 March 2019

Published online: 30 April 2019

References

- Cairns, R. A., Harris, I. S. & Mak, T. W. Regulation of cancer cell metabolism. *Nat. Rev. Cancer* **11**, 85–95 (2011).
- Yeung, S. J., Pan, J. & Lee, M.-H. Roles of p53, MYC and HIF-1 in regulating glycolysis—the seventh hallmark of cancer. *Cell. Mol. Life Sci.* **65**, 3981–3999 (2008).
- Zuzarte-Luis, V. & Mota, M. M. Parasite sensing of host nutrients and environmental cues. *Cell Host Microbe* **23**, 749–758 (2018).
- Tretina, K., Gotia, H. T., Mann, D. J. & Silva, J. C. *Theileria*-transformed bovine leukocytes have cancer hallmarks. *Trends Parasitol.* **31**, 306–314 (2015).
- Cock-Rada, A. M. et al. SMYD3 promotes cancer invasion by epigenetic upregulation of the metalloproteinase MMP-9. *Cancer Res.* **72**, 810–820 (2012).
- Dobbelaere, D. & Heussler, V. Transformation of leukocytes by *Theileria parva* and *T. annulata*. *Annu. Rev. Microbiol.* **53**, 1–42 (1999).
- Chaussepied, M. & Langsley, G. *Theileria* transformation of bovine leukocytes: a parasite model for the study of lymphoproliferation. *Res. Immunol.* **147**, 127–138 (1996).
- Medjkane, S., Perichon, M., Marsolier, J., Dairou, J. & Weitzman, J. B. *Theileria* induces oxidative stress and HIF1α activation that are essential for host leukocyte transformation. *Oncogene* **33**, 1809–1817 (2014).
- Cheeseman, K. & Weitzman, J. B. Host-parasite interactions: an intimate epigenetic relationship. *Cell Microbiol.* **17**, 1121–1132 (2015).

- Marsolier, J. et al. *Theileria* parasites secrete a prolyl isomerase to maintain host leukocyte transformation. *Nature* **520**, 378–382 (2015).
- Marsolier, J. et al. OncomiR addiction is generated by a miR-155 feedback loop in *Theileria*-transformed leukocytes. *PLoS Pathog.* **9**, e1003222 (2013).
- Yang, W. et al. ERK1/2-dependent phosphorylation and nuclear translocation of PKM2 promotes the Warburg effect. *Nat. Cell Biol.* **14**, 1295–1304 (2012).
- Luo, W. et al. Pyruvate kinase M2 is a PHD3-stimulated coactivator for hypoxia-inducible factor 1. *Cell* **145**, 732–744 (2011).
- Wang, H.-J. et al. JMJD5 regulates PKM2 nuclear translocation and reprograms HIF-1α-mediated glucose metabolism. *Proc. Natl Acad. Sci. USA* **111**, 279–284 (2014).
- Zhou, X. Z. et al. Pin1-dependent prolyl isomerization regulates dephosphorylation of Cdc25C and Tau proteins. *Mol. Cell* **6**, 873–883 (2000).
- Gillies, R. J., Robey, I. & Gatenby, R. A. Causes and consequences of increased glucose metabolism of cancers. *J. Nucl. Med.* **49**, 24S–42S (2008).
- Medjkane, S. & Weitzman, J. B. A reversible Warburg effect is induced by *Theileria* parasites to transform host leukocytes. *Cell Cycle* **12**, 2167–2168 (2013).
- Metheni, M., Lombes, A., Bouillaud, F., Batteux, F. & Langsley, G. HIF-1α induction, proliferation and glycolysis of *Theileria*-infected leukocytes. *Cell Microbiol.* **17**, 467–472 (2015).
- Dayton, T. L., Jacks, T. & Vander Heiden, M. G. PKM2, cancer metabolism, and the road ahead. *EMBO Rep.* **17**, 1721–1730 (2016).
- Yang, W. et al. Nuclear PKM2 regulates beta-catenin transactivation upon EGFR activation. *Nature* **480**, 118–122 (2011).
- Fritsch, L. et al. A subset of the histone H3 lysine 9 methyltransferases Suv39h1, G9a, GLP, and SETDB1 participate in a multimeric complex. *Mol. Cell* **37**, 46–56 (2010).

Acknowledgements

We thank members of the Weitzman laboratory for critical reading of the manuscript and invaluable advice on this study. We thank members of the UMR7216 for helpful discussions. We thank G. Langsley (Institut Cochin, Paris, France) for the generous gift of TBL3, BL3, and TpMD409 cells. This work was supported by the French National Research Agency (ANR) (Blanc 11-BSV3-016) and the Who Am I? Laboratory of Excellence #ANR-11-LABX-0071 funded by the French Government through its Investments for the Future program operated by the ANR under grant #ANR-11-IDEX-0005-01, the Fondation ARC pour la Recherche sur le Cancer (ARC n°155029), and the Institut Universitaire de France (IUF) (2012ND 3369).

Author contributions

J.B.W. and S.M. developed the concept and provided overall supervision. J.B.W., S.M., and J.M. designed the study, analysed the results and wrote the manuscript. S.M., M.P., and J.M. performed the experiments.


Additional information

Supplementary information accompanies this paper at <https://doi.org/10.1038/s42003-019-0386-6>.

Competing interests: The authors declare no competing interests.

Reprints and permission information is available online at <http://npg.nature.com/reprintsandpermissions/>

Publisher's note: Springer Nature remains neutral with regard to jurisdictional claims in published maps and institutional affiliations.

 **Open Access** This article is licensed under a Creative Commons Attribution 4.0 International License, which permits use, sharing, adaptation, distribution and reproduction in any medium or format, as long as you give appropriate credit to the original author(s) and the source, provide a link to the Creative Commons license, and indicate if changes were made. The images or other third party material in this article are included in the article's Creative Commons license, unless indicated otherwise in a credit line to the material. If material is not included in the article's Creative Commons license and your intended use is not permitted by statutory regulation or exceeds the permitted use, you will need to obtain permission directly from the copyright holder. To view a copy of this license, visit <http://creativecommons.org/licenses/by/4.0/>.

© The Author(s) 2019